

## Altered Enthalpy–Entropy Compensation in Picomolar Transition State Analogues of Human Purine Nucleoside Phosphorylase<sup>†</sup>

Achelle A. Edwards,<sup>‡</sup> Jennifer M. Mason,<sup>§</sup> Keith Clinch,<sup>§</sup> Peter C. Tyler,<sup>§</sup> Gary B. Evans,<sup>§</sup> and Vern L. Schramm<sup>\*,‡</sup>

<sup>‡</sup>*Department of Biochemistry, Albert Einstein College of Medicine, Bronx, New York 10461, and* <sup>§</sup>*Carbohydrate Chemistry Team, Industrial Research Ltd., Lower Hutt, New Zealand*

*Received April 6, 2009; Revised Manuscript Received May 8, 2009*

**ABSTRACT:** Human purine nucleoside phosphorylase (PNP) belongs to the trimeric class of PNPs and is essential for catabolism of deoxyguanosine. Genetic deficiency of PNP in humans causes a specific T-cell immune deficiency, and transition state analogue inhibitors of PNP are in development for treatment of T-cell cancers and autoimmune disorders. Four generations of Immucillins have been developed, each of which contains inhibitors binding with picomolar affinity to human PNP. Full inhibition of PNP occurs upon binding to the first of three subunits, and binding to subsequent sites occurs with negative cooperativity. In contrast, substrate analogue and product bind without cooperativity. Titrations of human PNP using isothermal calorimetry indicate that binding of a structurally rigid first-generation Immucillin ( $K_d = 56$  pM) is driven by large negative enthalpy values ( $\Delta H = -21.2$  kcal/mol) with a substantial entropic ( $-T\Delta S$ ) penalty. The tightest-binding inhibitors ( $K_d = 5$ –9 pM) have increased conformational flexibility. Despite their conformational freedom in solution, flexible inhibitors bind with high affinity because of reduced entropic penalties. Entropic penalties are proposed to arise from conformational freezing of the PNP·inhibitor complex with the entropy term dominated by protein dynamics. The conformationally flexible Immucillins reduce the system entropic penalty. Disrupting the ribosyl 5'-hydroxyl interaction of transition state analogues with PNP causes favorable entropy of binding. Tight binding of the 17 Immucillins is characterized by large enthalpic contributions, emphasizing their similarity to the transition state. Via introduction of flexibility into the inhibitor structure, the enthalpy–entropy compensation pattern is altered to permit tighter binding.

Human purine nucleoside phosphorylase (PNP) is required for the catabolism of 6-oxynucleosides (and 2'-deoxynucleosides) to free nucleobases for recycling by phosphoribosyl transferases or oxidation to uric acid and excretion. Genetic deficiency of PNP in humans causes deoxyguanosine accumulation in the blood, and its conversion to dGTP causes arrest of DNA synthesis and apoptosis specifically in activated T-cells. Human PNP is therefore a target for the treatment of autoimmune disorders and T-cell cancers (1, 2).

The transition state structure of human PNP has permitted the design of several transition state analogues with picomolar dissociation constants (3–7). The transition state is characterized by a fully developed ribocation with a C1'–N9 distance of  $\geq 3.0$  Å and the phosphate nucleophile at a similar distance from C1' of the ribosyl cation (Figure 1) (3). Four structurally distinct generations of transition state analogues have been synthesized (Figure 2). The first-generation inhibitor, Immucillin-H (2, Table 1), was designed to mimic the early dissociative transition state of bovine PNP (8, 9). Immucillin-H [(1S)-1-(9-deazahypoxanthin-9-yl)-1,4-dideoxy-1,

4-imino-D-ribose] binds with a  $K_d$  of 23 pM to the bovine enzyme and with a slightly higher  $K_d$  of 56 pM to human PNP (4, 9). The fully dissociative ( $S_N1$ ) transition state of human PNP led to the second-generation DADMe-Immucillins [4'-deaza-1'-aza-2'-deoxy-1'-(9-methylene)-Immucillins]. These include a methylene bridge between the hydroxypyrrolidine mimic of the ribocation and the 9-deazapurine to mimic the fully dissociative transition state of human PNP. DADMe-Immucillin-H (6, Table 1) binds tightly to human PNP, giving a dissociation constant of 8.5 pM (5, 10). The third generation of Immucillins has the ribose ring replaced with an acyclic, chiral ribocation mimic (the acyclic chiral imino alcohols). The tightest-binding inhibitor in this group is DATMe-Immucillin-H (8, Table 1) with a dissociation constant of 8.6 pM for human PNP (5). The fourth-generation transition state analogues for human PNP are represented by SerMe-Immucillin-H (4, Table 1), an acyclic, achiral mimic of the ribocationic transition state with a dissociation constant of 5.2 pM for human PNP (7). Complete inhibition of trimeric PNP occurs when transition state analogues bind to only one of the three catalytic sites (9). X-ray structures of PNPs with substrate, product, or inhibitor complexes reveal that all sites are filled under ligand saturation (11–13). Thermodynamic parameters for Immucillin binding have not been reported; however, those for the

<sup>†</sup>Supported by National Institutes of Health Grant GM41916.

<sup>\*</sup>To whom correspondence should be addressed. E-mail: vern@aeom.yu.edu. Telephone: (718) 430-2813. Fax: (718) 430-8565.

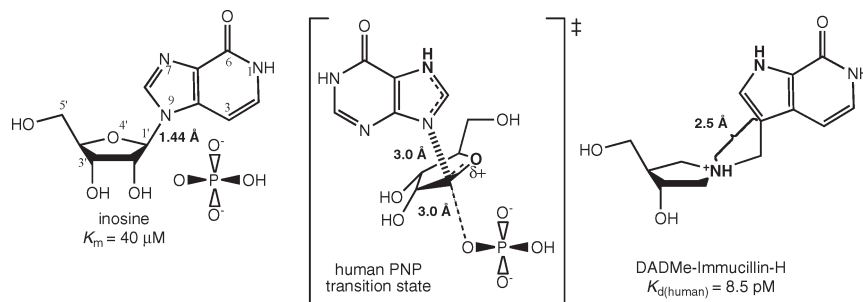


FIGURE 1: Reactants, transition state structure, and a transition state analogue of human PNP. Key features of the human PNP transition state include N7 protonation, formation of a ribocation, the 3.0 Å C1'–N9 distance, and the phosphate nucleophile a similar distance from the ribosyl group. This led to the development of the DADMe-Immucillins. The 9-deazahypoxanthine group provides N7 protonation and chemical stability. A methylene bridge provides the extended geometry, and placing the nitrogen at the 1'-position in the pyrrolidine ring provides the electronic mimic of the fully dissociative transition state of human PNP. Human PNP also uses 2'-deoxyinosine as a substrate, justifying the 2'-deoxy structure in the DADMe-Immucillin-H transition state analogue.

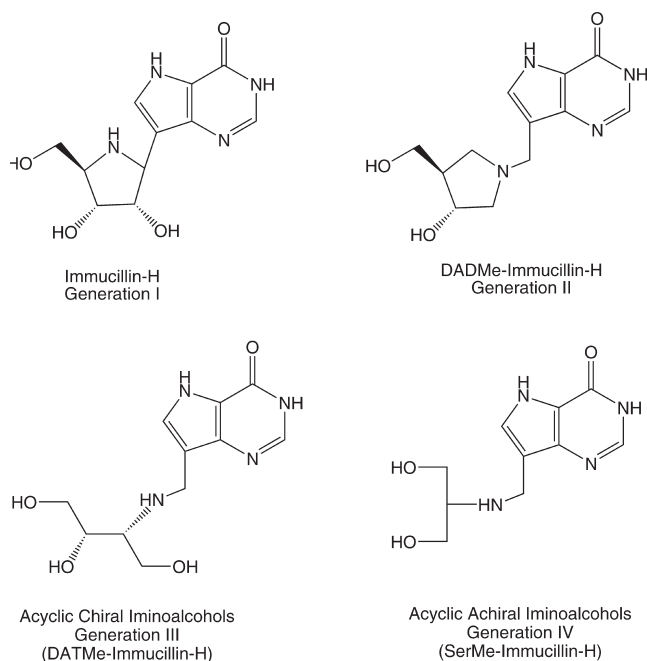


FIGURE 2: Four generations of PNP transition state analogue inhibitors. Immucillin-H was designed to mimic the bovine PNP transition state. DADMe-Immucillin-H is a mimic of the human PNP transition state. The acyclic, chiral imino alcohols provide the three hydroxyl groups found in Immucillin-H and the amino cation functionality to mimic features of the fully dissociated transition state of human PNP. The acyclic, achiral imino alcohols provide the two hydroxyl groups as in DADMe-Immucillin-H and provide ease of synthesis. These inhibitors have dissociation constants in the picomolar range (see Table 1).

binding of product and multisubstrate analogue inhibitors to bovine PNP have been published (e.g., ref (14)). Here, four generations of transition state analogues and related inhibitors were titrated against human PNP using isothermal titration calorimetry (ITC). Transition state analogue binding to the catalytic sites of PNP occurs with strong negative cooperativity. In contrast, binding of 9-deazainosine, a substrate analogue inhibitor, and hypoxanthine, a product, reveals normal binding isotherms, clearly distinguishing the nature of transition state and ground state interactions.

## MATERIALS AND METHODS

**Enzyme Purification and Preparation.** His-tagged human PNP was expressed in *Escherichia coli* and prepared in a manner

similar to published procedures (3). Briefly, cells were grown at 37 °C overnight in two 100 mL portions of LB medium with ampicillin (100 µg/mL). This was used to inoculate 40 L of LB medium containing ampicillin and the mixture allowed to achieve an OD<sub>600</sub> of 0.4–0.6 (3–4 h). Expression was induced with IPTG (1 mM) for 4 h at 37 °C. Cells were pelleted and resuspended in 300 mL of 5 mM imidazole, 500 mM NaCl, 20 mM Tris-HCl buffer (pH 8.0), protease inhibitor (four tablets of EDTA-free protease inhibitor from Roche Diagnostics), and approximately 1 mg each of DNase I (from bovine pancreas) (Roche Diagnostics) and lysozyme (from chicken egg white) (Sigma-Aldrich). Cells were disrupted twice with a French press. The supernatant from centrifugation (39000g for 30 min) was applied to a 50 mL column of Ni-NTA resin (QIAGEN) previously equilibrated with 3 column volumes of 5 mM imidazole, 500 mM NaCl, and 20 mM Tris-HCl buffer (pH 8.0). After the sample had been washed [3 column volumes of 20 mM imidazole, 10 mM NaCl, and 0.4 mM Tris-HCl buffer (pH 8.0)], His-tagged human PNP was eluted with a 2 to 40% gradient of 1 M imidazole, 500 mM NaCl, and 20 mM Tris-HCl buffer (pH 8.0) in water on an AKTA FPLC system (GE Healthcare). Fractions of pure human PNP (by SDS-PAGE) were concentrated to approximately 50 mL by AMICON ultrafiltration and dialyzed against 20 mM Tris-HCl (pH 8.0, 48 h) to give approximately 24 mg/mL PNP. Plastic tubes containing 1.8 mL were frozen rapidly in liquid nitrogen and stored at –80 °C. Human PNP prepared by this method has two-thirds of its sites occupied with hypoxanthine. Removal of hypoxanthine was effected by incubation in 100 mM KH<sub>2</sub>PO<sub>4</sub> containing 10% (w/v) charcoal for 5 min followed by centrifugation and filtration (15). Enzyme recovery is typically 80%, and the steady state kinetic properties of the enzyme are unaffected by charcoal treatment.

**Inhibitors.** The Immucillins were prepared and provided as generous gifts by P. C. Tyler and G. B. Evans of the Carbohydrate Chemistry Team, Industrial Research Ltd. (e.g., refs (4), (6), and (10)). Immucillins 13 and 14 were prepared from (3R,4R)- and (3S,4S)-1-benzylpyrrolidinediol, respectively, purchased from Aldrich Chemical Co. The benzyls were removed by hydrogenolysis, and the resulting amines were treated with 9-deazahypoxanthine and formaldehyde in a Mannich reaction in the same manner we have reported previously to give the substituted 9-deazahypoxanthines (16). 9-Deazainosine was the generous gift of B. A. Otter and R. S. Kline (Montefiore Medical Center, Bronx, NY) (17).

Table 1: Thermodynamics for Binding the Immucillins to the First Subunit of Human PNP Arranged in Order of Increasing Entropy (negative to positive  $\Delta S$ )

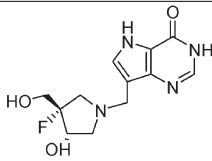
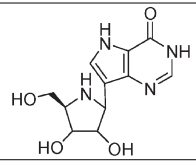
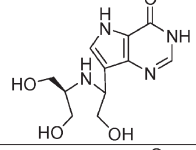
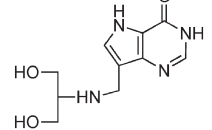
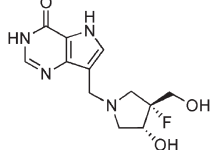
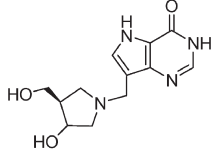
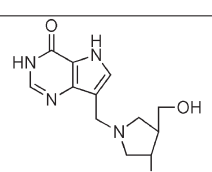
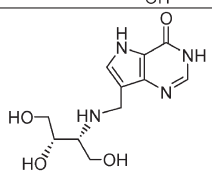
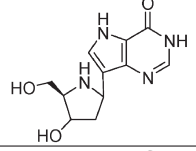
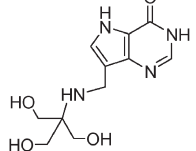
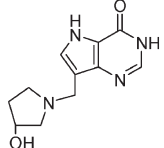
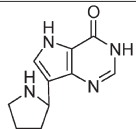
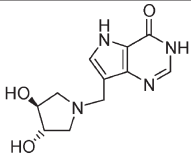
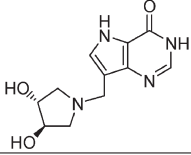
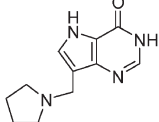
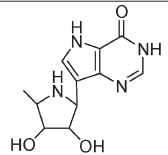
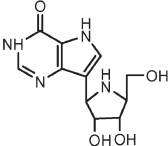
entry	structure	$K_d$ (pM) <sup>a</sup>	$\Delta G$ (kcal/mol) <sup>b</sup>	$\Delta H$ (kcal/mol) <sup>c</sup>	$-T\Delta S$ (kcal/mol) <sup>d</sup>
1		$32 \pm 10^e$	$-14.4 \pm 0.3$	$-22.7 \pm 0.4$	$8.3 \pm 0.5$
2		$56 \pm 15^f$	$-14.1 \pm 0.3$	$-21.2 \pm 0.2$	$7.1 \pm 0.4$
3		$210 \pm 80^g$	$-13.3 \pm 0.4$	$-20.4 \pm 0.2$	$7.1 \pm 0.4$
4		$5.2 \pm 0.4^h$	$-15.5 \pm 0.1$	$-20.2 \pm 0.2$	$4.7 \pm 0.2$
5		$1820 \pm 80^e$	$-12.0 \pm 0.04$	$-15.6 \pm 0.1$	$3.6 \pm 0.1$
6		$8.5 \pm 0.2^g$	$-15.1 \pm 0.02$	$-18.6 \pm 0.4$	$3.5 \pm 0.4$
7		$380 \pm 30^i$	$-12.9 \pm 0.1$	$-16.1 \pm 0.2$	$3.2 \pm 0.2$
8		$8.6 \pm 0.6^g$	$-15.2 \pm 0.1$	$-17.5 \pm 0.2$	$2.3 \pm 0.2$
9		$140 \pm 10^j$	$-13.5 \pm 0.1$	$-15.2 \pm 0.5$	$1.7 \pm 0.5$
10		$620 \pm 170^k$	$-12.6 \pm 0.3$	$-13.3 \pm 0.5$	$0.7 \pm 0.6$
11		$383 \pm 6$	$-12.9 \pm 0.02$	$-12.8 \pm 0.9$	$-0.1 \pm 0.9$

Table 1: Continued

entry	structure	$K_d$ (pM) <sup>a</sup>	$\Delta G$ (kcal/mol) <sup>b</sup>	$\Delta H$ (kcal/mol) <sup>c</sup>	$-T\Delta S$ (kcal/mol) <sup>d</sup>
12		840000 ± 110000 <sup>e</sup>	-8.3 ± 0.1	-7.4 ± 0.3	-0.9 ± 0.3
13		156 ± 72	-13.5 ± 0.5	-12.3 ± 0.3	-1.2 ± 0.6
14		53000 ± 2000	-10.0 ± 0.04	-8.6 ± 1.0	-1.4 ± 1.0
15		5500 ± 900 <sup>f</sup>	-11.3 ± 0.2	-9.6 ± 0.2	-1.7 ± 0.3
16		25000 ± 1000 <sup>g</sup>	-10.4 ± 0.04	-8.5 ± 0.2	-1.9 ± 0.2
17		12000 ± 2000 <sup>h</sup>	-10.9 ± 0.2	-8.4 ± 0.2	-2.5 ± 0.3

<sup>a</sup> Inhibition assays were performed in 50 mM KH<sub>2</sub>PO<sub>4</sub> at pH 7.4 and 25 °C. <sup>b</sup> The  $\Delta G$  values were calculated from the inhibition constants using the equation  $\Delta G = RT \ln K_d$ . <sup>c</sup> The  $\Delta H$  values were determined from ITC titrations of a single subunit on the enzyme in 50 mM KH<sub>2</sub>PO<sub>4</sub> at pH 7.4 and 27 °C. <sup>d</sup> The Gibbs free energy equation was used to calculate  $-T\Delta S$ . <sup>e</sup> From ref (6). <sup>f</sup> From ref (4). <sup>g</sup> From ref (5). <sup>h</sup> From ref (7). <sup>i</sup> From ref (38). <sup>j</sup> From ref (10). <sup>k</sup> From ref (39).

**Enzymatic and Inhibition Assays.** PNP catalytic activity with inosine as the substrate monitored conversion of hypoxanthine to uric acid ( $\epsilon_{293} = 12900 \text{ M}^{-1} \text{ cm}^{-1}$ ) in a coupled assay containing 0.5 nM PNP, 50 mM potassium phosphate (pH 7.4), and 60 milliunits of xanthine oxidase (from milk, 2.6 M ammonium sulfate suspension) (Sigma-Aldrich) (9). Slow-onset inhibition was assessed by addition of enzyme (0.2 nM) to complete assay mixtures with  $\geq 1$  mM inosine and varied inhibitor concentrations. Concentrations were determined from the extinction coefficients [human PNP  $\epsilon_{280} = 28830 \text{ M}^{-1} \text{ cm}^{-1}$  (Protparam, www.expasy.org); Immucillins  $\epsilon_{261} = 9540 \text{ M}^{-1} \text{ cm}^{-1}$ ] (17). The inhibitor concentration was at least 10-fold greater than the enzyme concentration, as required for simple analysis of slow-onset tight-binding inhibition (18). Rates were monitored for 2 h to determine the initial reaction rate and slow-onset inhibition (final reaction rate) (9). The  $K_i$  or  $K_i^*$  values were determined by fitting the initial and/or final steady state rates and inhibitor concentrations to the expression

$$V_i/V_o = [S]/(K_M + [S] + K_M[I]/K_i)$$

where  $V_i$  and  $V_o$  are initial (for  $K_i$ ) and final (for  $K_i^*$ ) steady state rates in the presence and absence of inhibitor, respectively,  $K_M$  is the Michaelis constant for inosine,  $[I]$  is the free inhibitor

concentration, and  $[S]$  is the substrate concentration.  $K_i^*$  or  $K_i$  values (if no slow onset occurred) are reported as the dissociation constants (e.g., Table 1).

**Isothermal Titration Calorimetry Studies.** (i) *Single-Subunit Titrations.* Calorimetric titrations of PNP with the Immucillins were performed on a VP-ITC microcalorimeter (MicroCal). Protein samples were dialyzed against 50 mM potassium phosphate buffer (pH 7.4). Ligand solutions were dissolved in dialysate and filtered (Millipore 0.2  $\mu\text{m}$ ) and the ligand and protein solutions degassed (Microcal Thermovac) for 5 min prior to titrations. The 1.46 mL sample cell was filled with an approximately 30  $\mu\text{M}$  PNP (monomer) solution and the injection syringe with an  $\sim 450 \mu\text{M}$  ligand solution.

Single-subunit titrations involved seven or eight 4  $\mu\text{L}$  injections. Each titration was performed six times to obtain an average of the  $\Delta H$  values.  $\Delta G$  was based on  $K_i$  values from inhibition assays described above, and the  $-T\Delta S$  term was calculated from the Gibbs free energy expression

$$\Delta G = \Delta H - T\Delta S \quad (1)$$

(ii) *Trimer Titrations.* Titrating the PNP trimer with Immucillins used 30–35 injections at a rate of 4  $\mu\text{L}$  every 3 min. The data were fit to independent and/or sequential sites

models for three binding sites to give the thermodynamic parameters  $\Delta G$ ,  $\Delta H$ , and  $-T\Delta S$ . When the sequential sites model was used to fit the data, the stoichiometry for binding is assumed to be one per binding site.

Titration of the trimer with 9-deazainosine and hypoxanthine ( $\sim 700 \mu\text{M}$  in the injector) used 20–50  $\mu\text{M}$  PNP and involved 30–60 injections. The data were fit to the independent sites model to yield the thermodynamic parameters and an estimate for the stoichiometry of binding,  $N$ .

(iii) *Data Fitting*. The equation used to fit data to independent binding sites (used to fit 9-deazainosine and hypoxanthine binding isotherms) is  $K = \Theta/(1 - \Theta)[L]$ , where  $K$  is the binding constant,  $\Theta$  is the fraction of sites occupied by ligand  $L$ , and  $[L]$  is the free ligand concentration and

$$Q = (NM_t\Delta H V_0/2)\{1 + L_t/NM_t + 1/NKM_t - \sqrt{[(1 + L_t/NM_t + 1/NKM_t)^2 - 4L_t/NM_t]}\}$$

where  $Q$  is the total heat,  $N$  is the stoichiometry,  $M_t$  is the total PNP concentration, and  $L_t$  is the total ligand concentration. The equation used to fit data to three interdependent binding sites (used to fit the binding isotherms of Immucillins **5** and **15**) is

$$\begin{aligned} K_1 &= [\text{ML}]/[\text{M}][\text{L}]; K_2 = [\text{ML}_2]/[\text{ML}][\text{L}]; \\ K_3 &= [\text{ML}_3]/[\text{ML}_2][\text{L}] \\ Q &= M_t V_0 [F_1 \Delta H_1 + F_2 (\Delta H_1 + \Delta H_2) + \\ &\quad F_3 (\Delta H_1 + \Delta H_2 + \Delta H_3)] \end{aligned}$$

where  $F_i$  is the fraction of PNP having  $i$  bound ligands

$$\begin{aligned} F_0 &= 1/P; F_1 = K_1[L]/P; F_2 = K_1 K_2 [L]^2/P; \\ F_3 &= K_1 K_2 K_3 [L]^3/P \end{aligned}$$

$$P = 1 + K_1[L] + K_1 K_2 [L]^2 + K_1 K_2 K_3 [L]^3$$

and the heat change in each case is given by

$$\Delta Q(i) = Q(i) + dV_i/2V_0[Q(i) + Q(i-1)] - Q(i-1)$$

where  $\Delta Q(i)$  is the heat released from the  $i$ th injection,  $Q(i)$  is the total heat content,  $dV_i$  is the injection volume, and  $V_0$  is the active cell volume

(iv) *Competitive ITC*. Competitive titrations were used to determine the thermodynamics for binding of Immucillin **2** to the PNP trimer. The enzyme was first titrated with a weaker ligand (Immucillin **15** or 9-deazainosine) followed by displacement titration with Immucillin **2** (a tight ligand) to give apparent  $K_d$  and  $\Delta H$  values (eqs 2 and 3). A separate titration of PNP with Immucillin **2** was used with the following equations to determine the  $K_{\text{dtight}}$  and  $\Delta H_{\text{tight}}$  values for binding of Immucillin **2** to all three sites of human PNP (19, 20).

$$\begin{aligned} \Delta H_{\text{app}} &= \Delta H_{\text{tight}} - \\ \Delta H_{\text{weak}} &[(K_{\text{weak}}[\text{ligand}_{\text{weak}}])/(1 + K_{\text{weak}}[\text{ligand}_{\text{weak}}])] \quad (2) \\ K_{\text{app}} &= K_{\text{tight}}/(1 + K_{\text{weak}}[\text{ligand}_{\text{weak}}]) \quad (3) \end{aligned}$$

where  $\Delta H_{\text{app}}$ ,  $\Delta H_{\text{tight}}$ , and  $\Delta H_{\text{weak}}$  are the apparent enthalpy of the displacement ITC, the enthalpy change for the tight Immucillin **2**, and the enthalpy change for the weak ligand,

respectively.  $K_{\text{app}}$ ,  $K_{\text{tight}}$ , and  $K_{\text{weak}}$  are the apparent  $K$  values for displacement ITC, the  $K$  of the tight ligand, and the  $K$  of the weak ligand, respectively;  $[\text{ligand}_{\text{weak}}]$  is the free concentration of the preequilibrated weaker-binding ligand.

(v) *Control Experiments*. Control ITC experiments involved titration of ligand into the buffer solution with correction for any heat change using the “subtract reference” function in Origin 7.0. Another control involved titration of the working solution of PNP with Immucillin **2** each day before the start of other titrations. This analysis ensured the protein was fully active for each titration.

## RESULTS

*Immucillin Binding to the First Catalytic Site of Human PNP*. Substoichiometric titration of Immucillins **2**, **8**, **10**, and **15** into the first catalytic site of human PNP caused a constant enthalpy change per injection (Figure 3). The  $\Delta H$  for binding to the first subunit is calculated from the average of these values (Table 1). Enthalpy changes for these four Immucillins are large and exothermic, from  $-9.6$  to  $-21.2$  kcal/mol (Table 1 and Figure 3). Accurate  $K_d$  values are known from kinetic studies (e.g., refs (5) and (10)) for these and other Immucillins, permitting resolution of the thermodynamic constants for binding to the first catalytic site of this homotrimer. The same approach was used to establish thermodynamic parameters ( $\Delta H$ ,  $-T\Delta S$ , and their contribution to  $\Delta G$ ) for binding of 17 Immucillins to human PNP, arranged in order of  $T\Delta S$  values (Table 1 and Figure 4). Immucillin binding to human PNP is characterized by  $\Delta G$  values dominated by the enthalpy term, with enthalpies from  $-7.4$  (Immucillin **12**) to  $-22.7$  kcal/mol (Immucillin **1**). Entropy changes ( $-T\Delta S$ ) vary from unfavorable (Immucillins **1–9**) to slightly favorable (Immucillins **13–17**), and several Immucillins (**10–12**) bind with entropy changes near zero. The most tightly binding Immucillins (**4**, **6**, and **8**) are enthalpy-driven with relatively small penalties in the entropy terms. The relative enthalpy and entropy values for Immucillin binding demonstrate an enthalpy–entropy compensation effect (21–25) (Figure 5). Immucillins with the largest favorable enthalpic values (Immucillins **1–9**) also exhibit unfavorable entropy changes. Immucillins with favorable entropy changes (Immucillins **13–17**) also have less favorable enthalpic values and, consequently, bind more weakly. Immucillins **4**, **6**, and **8** reveal less than expected unfavorable entropy terms from a standard enthalpy–entropy compensation plot (Figure 5) and therefore exhibit unusually tight (picomolar) dissociation constants.

*Immucillins Bind to Three Sites with Negative Cooperativity*. Human PNP is a homotrimer, and binding of Immucillins **2**, **5**, and **15** indicated a stoichiometry of three sites on human PNP and could not be fit to simpler models (Table 2 and Figure 6). Binding of Immucillin **2** is 56 pM for the first catalytic site (Table 1) and demonstrates negative cooperativity at subsequent sites (Figure 6). The tight binding precludes fits of the data to the three-site model, but midpoint analysis for sites 2 and 3 permits estimates of enthalpy changes as these sites are filled. The  $\Delta H$  for first-site binding is  $-21.2$  kcal/mol (Table 1), and as sites 2 and 3 are titrated, the  $\Delta H$  values at their midpoints are  $-17.8$  and  $-13.7$  kcal/mol, respectively (Figure 6). Thus, values of 3.4 and 7.5 kcal/mol are lost from the cooperative binding enthalpy. The  $K_d$  values are not available for sites 2 and 3 from this data, but if it is assumed that the  $-T\Delta S$  term remains at 7.1 kcal/mol for second- and third-site binding, the  $K_{d2}$  for the



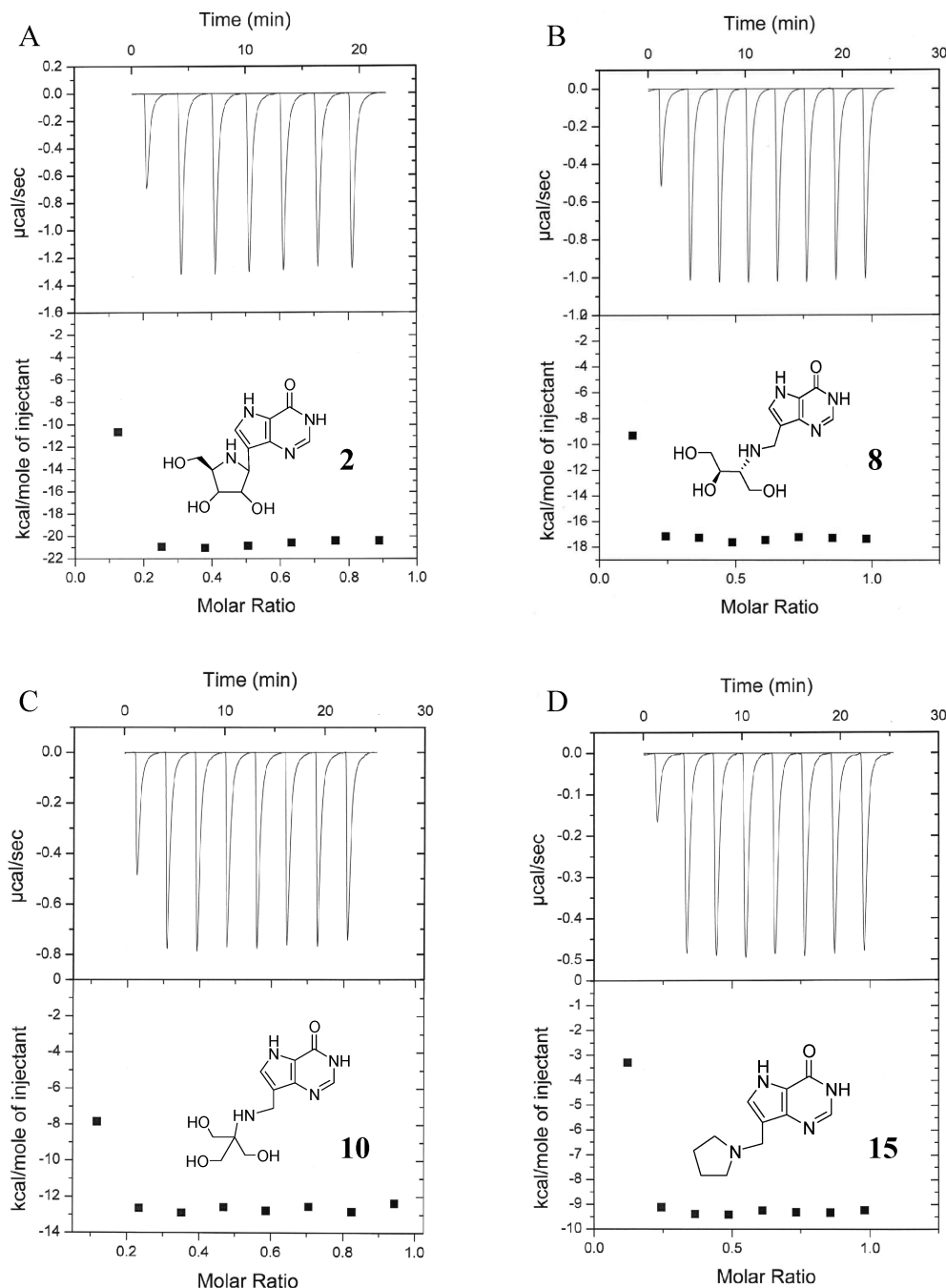


FIGURE 3: Single-subunit substoichiometric titrations of human PNP with Immucillins **2** (A), **8** (B), **10** (C), and **15** (D). Titrations provide enthalpic values for inhibitor binding to the first catalytic site of PNP.  $\Delta G$  values are known from kinetic experiments, and the  $T\Delta S$  can be calculated to provide the values listed in Table 1. With picomolar to low nanomolar inhibitor dissociation constants and PNP subunit concentrations near 30  $\mu\text{M}$ , there is no significant accumulation of free inhibitor during these substoichiometric titrations.

second site can be estimated to be 16 nM, more than 200-fold weaker than that for binding of **2** to the first site. Likewise, binding at the third site can be estimated to be 15  $\mu\text{M}$  by the same approximation, but this is likely a poor approximation because of altered entropy as affinity changes. We explored third-site affinity by competitive binding experiments (see below).

Immucillins **5** and **15** also provide examples of negative cooperativity in binding to the three catalytic sites. When the values for  $K_{d1}$  are fixed from the results of Table 1 and the data for full three-site titration fit to three cooperative sites, thermodynamic values can be estimated for binding to sites 2 and 3. Immucillin **5** binds to the first site with a  $K_{d1}$  of 1.8 nM ( $\Delta G = -12$  kcal/mol,  $\Delta H = -15.5$  kcal/mol, and  $-T\Delta S = 3.5$  kcal/mol)

and to the third site with a  $K_{d3}$  of 667 nM ( $\Delta G = -8.5$  kcal/mol,  $\Delta H = -8.4$  kcal/mol, and  $-T\Delta S = -0.1$  kcal/mol). Immucillin **15** binds to the first site with a  $K_{d1}$  of 5.5 nM ( $\Delta G = -11.3$  kcal/mol,  $\Delta H = -9.0$  kcal/mol, and  $-T\Delta S = -2.3$  kcal/mol) and to the third site with a  $K_{d3}$  of 402 nM ( $\Delta G = -8.8$  kcal/mol,  $\Delta H = -1.5$  kcal/mol, and  $-T\Delta S = -7.3$  kcal/mol). Immucillin **5** binds with a 370-fold affinity difference for first- and third-site binding to give a  $\Delta\Delta G$  of 3.5 kcal/mol, a  $\Delta\Delta H$  of 7.1 kcal/mol, and a  $\Delta(-T\Delta S)$  of  $-3.6$  kcal/mol. Immucillin **15** binds to the trimer with a 73-fold affinity difference between the first and third sites, a  $\Delta\Delta G$  of 2.5 kcal/mol, a  $\Delta\Delta H$  of 7.5 kcal/mol, and a  $\Delta(-T\Delta S)$  of  $-5.0$  kcal/mol. Sequential binding of Immucillins **5** and **15** to human PNP results in Gibbs free energy and enthalpy changes that

become less favorable as sites are filled. However, as enthalpy changes become less exothermic, entropy changes become more favorable, in keeping with the enthalpy–entropy compensation effect.

**Competitive ITC.** Immucillin **2** binds with a dissociation constant of 56 pM at the first binding site, and competitive ITC was used to alter the apparent binding parameters to permit more complete analysis of thermodynamic constants. The relatively weakly bound Immucillin **15** was used to fully saturate the catalytic sites and thereby provide displacement ligands for the more tightly bound Immucillin **2**. Titration of PNP with Immucillin **15** [ $K_d = 5.5$ , 55, and 402 nM for the first, second, and third sites, respectively (Tables 1 and 2)] was followed by a displacement titration in which Immucillin **2** ( $K_d = 56$  pM for the

first site) displaced Immucillin **15**. Titration of Immucillin **2** into unliganded PNP provides only estimates for  $K_{d2}$  and  $K_{d3}$  (see above and Figure 6). Displacement of the PNP·Immucillin **15**·PO<sub>4</sub> complex with Immucillin **2** follows a normal binding isotherm and gives a competitive  $K_d$  of 12 nM at each of the three sites [ $\Delta H = -12.9$  and  $-T\Delta S = 2.0$  kcal/mol (Figure 6 and Table 2)]. The normal binding isotherm indicates that saturation of sites with Immucillin **15** has completed the cooperative transition. With a displacement  $K_d$  of 12 nM for Immucillin **2** and a first-site  $K_d$  of 56 pM for this ligand, the difference between first- and third-site binding affinity is approximately 214-fold.

The constants obtained by displacement of **15** represent the affinity of **2** for the first binding site when the remaining two sites are filled with **15**. These thermodynamic constants establish a decreased affinity transmitted from sites 2 and 3 which remain filled with **15** as the first site is filled with **2** (Table 2). In contrast, as the third site is filled by **2** with displacement of the last remaining Immucillin **15**, the first two sites are filled with **2** to make the binding of **2** to the final site a true  $K_d$  for PNP fully saturated with **2**. Thus, the intrinsic binding difference between sites 1 and 3 for binding of Immucillin **2** is 214-fold. In kinetic studies, filling the first site with **2** causes complete inhibition of PNP; therefore, filling the second and third sites is kinetically silent, but the relative affinities are resolved here by the competitive binding approach.

Negative cooperativity for **2** between sites 1 and 3 is caused by a change in thermodynamic interactions. Thus, binding of **2** at the first site is an enthalpic event ( $-21.2$  kcal/mol) causing a large loss in entropic freedom (7.1 kcal/mol). Binding of **2** to the third site shows strongly altered thermodynamic properties with an enthalpy of  $-12.9$  kcal/mol and a small entropic penalty of 2.0 kcal/mol. This difference in binding thermodynamics establishes large protein structural reorganization forces driven by transition state mimic contacts at sites 1 and 2.

**Binding 9-Deazainosine and Hypoxanthine to Human PNP.** A nonreactive substrate analogue of inosine, 9-deazainosine, binds to human PNP with an average affinity of 5.4  $\mu$ M

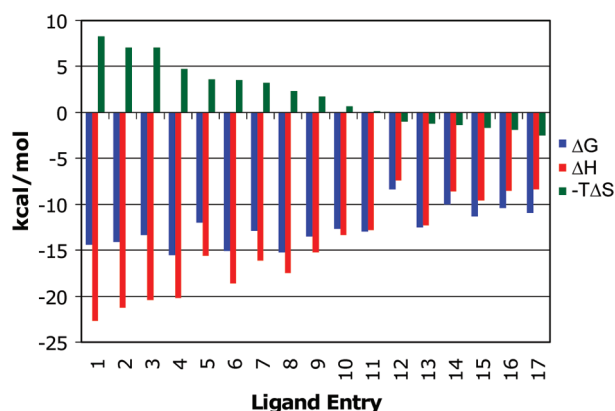


FIGURE 4: Thermodynamic signatures of Immucillins binding to the first subunit of human PNP (from Table 1):  $\Delta G$  (blue),  $\Delta H$  (red), and  $-T\Delta S$  (green). The most tightly bound Immucillins are characterized by enthalpy-driven binding with smaller entropic penalties (Immucillins **1–9**). Several Immucillins bind with near-zero entropy (Immucillins **10–12**). Immucillins with favorable entropy (Immucillins **13–17**) lack the 5'-hydroxyl group, known to interact with catalytically important His257 and to be involved in catalytic site dynamic motion.

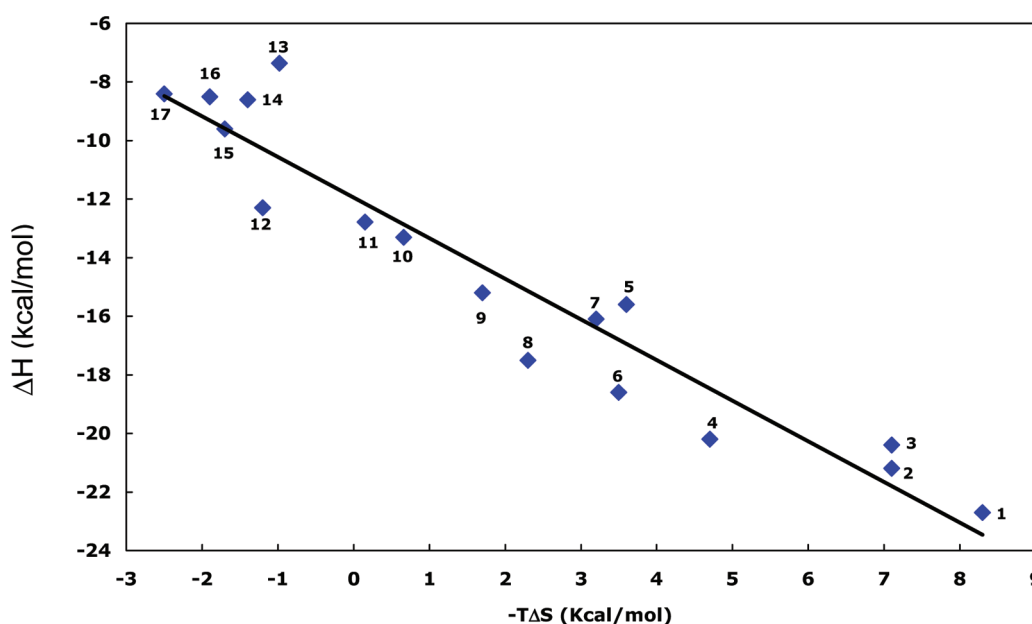
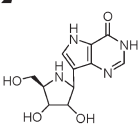
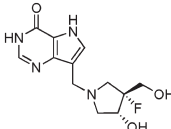
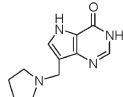


FIGURE 5: Enthalpy–entropy compensation for Immucillin binding to the first subunit of trimeric human PNP. The numbers correspond to the Immucillins in Table 1. Ligands that bind with the most favorable enthalpy (**1–3**) also have the largest unfavorable entropy. Immucillins **4**, **6**, and **8** exhibit lower-than-expected unfavorable entropies and are the most tightly bound species. Ligands with favorable entropic contributions (**12–17**) lack the ability to form a normal 5'-hydroxyl interaction at the catalytic site.

Table 2: Thermodynamics for Binding of Immucillins **2**, **5**, and **15** to All Three Subunits of Human PNP<sup>a</sup>

<b>2<sup>b</sup></b> 	$K_d$ (nM)	$12.0 \pm 3.3$		
	$\Delta G$ (kcal/mol)	$-10.9 \pm 0.2$		
	$\Delta H$ (kcal/mol)	$-12.9 \pm 0.6$		
	$-T\Delta S$ (kcal/mol)	$2.0 \pm 0.6$		
<b>5<sup>c</sup></b> 		1 <sup>st</sup> Site	2 <sup>nd</sup> Site	3 <sup>rd</sup> Site
	$K_d$ (nM)	$1.8 \pm 0.1^d$	$64 \pm 16$	$667 \pm 62$
	$\Delta G$ (kcal/mol)	$-12.0 \pm 0.1$	$-9.9 \pm 0.3$	$-8.5 \pm 0.1$
	$\Delta H$ (kcal/mol)	$-15.5 \pm 0.1$	$-13.7 \pm 0.2$	$-8.4 \pm 0.2$
<b>15<sup>c</sup></b> 	$K_d$ (nM)	$5.5 \pm 0.9^d$	$55 \pm 13$	$402 \pm 106$
	$\Delta G$ (kcal/mol)	$-11.3 \pm 0.2$	$-10.0 \pm 0.2$	$-8.8 \pm 0.3$
	$\Delta H$ (kcal/mol)	$-9.0 \pm 0.1$	$-5.0 \pm 0.2$	$-1.5 \pm 0.2$
	$-T\Delta S$ (kcal/mol)	$-2.3 \pm 0.2$	$-5.0 \pm 0.3$	$-7.3 \pm 0.4$

<sup>a</sup>ITC titrations were conducted in 50 mM KH<sub>2</sub>PO<sub>4</sub> at pH 7.4 and 27 °C. <sup>b</sup>The thermodynamics for binding Immucillin **2** were determined using a competitive titration and reflect average values for the three sites (see Figure 6). <sup>c</sup>The data were fit using the three-site sequential model provided in Origin 7.0. <sup>d</sup> $K_d$  values were determined from kinetic inhibition assays described in Materials and Methods.

( $\Delta G = -7.2$  kcal/mol). The binding is strongly enthalpy driven ( $\Delta H = -15.9$  kcal/mol) with entropic compensation reducing most of the enthalpy change ( $-T\Delta S = 8.7$  kcal/mol). This binding fits to an independent binding sites model but indicates a total binding stoichiometry of approximately two sites. Thus, binding to the third site differs in a significantly weaker affinity or a near-zero enthalpic change (Figure 7 and Table 3). This departure of the third binding site from the first two is also seen in **15** binding, where sites 1 and 2 are enthalpy-driven and site 3 is entropy-driven (Tables 1 and 2).

Binding of hypoxanthine is similar to that of 9-deazainosine with independent binding at two sites with an average affinity of 4.3  $\mu$ M ( $\Delta G = -7.2$  kcal/mol) and no enthalpic evidence for binding at the third catalytic site. Hypoxanthine binding differs from 9-deazainosine binding with an extreme enthalpy change ( $-30.5$  kcal/mol) combined with a large and unfavorable entropic component ( $-T\Delta S = 23.1$  kcal/mol) (Figure 7 and Table 3). Trimeric PNPs are isolated with 2 mol of tightly bound hypoxanthine, and in the case of the bovine PNP, the  $K_d$  value has been estimated to be 2 pM for the binary PNP·hypoxanthine complex, an affinity that decreases substantially in the presence of phosphate (26).

Competitive binding of Immucillin **2** to PNP saturated with 9-deazainosine differs substantially from the displacement of Immucillin **15**. 9-Deazainosine is isosteric with Immucillin **2**, differing only in the substitution of the 4'-oxygen with nitrogen and differing from substrate only in the replacement of N9 with C9 (Table 3). Titration of Immucillin **2** into the PNP·9-deazainosine·PO<sub>4</sub> complex occurs with high affinity at all three catalytic sites since no slope change occurs in the ITC titration plots until all three sites are filled (Figure 7). 9-Deazainosine binding occurs with a  $\Delta H$  of  $-15.9$  kcal/mol and a  $-T\Delta S$  of 8.7 kcal/mol. When Immucillin **2** displaces 9-deazainosine, an additional  $-8.3$  kcal/mol of  $\Delta H$  occurs. Since fully occupied enzyme is present throughout the displacement experiment, small entropic terms are expected and the anticipated binding energy would include the  $\Delta G$  for 9-deazainosine in addition to the  $\Delta H$  for **2** displacement of 9-deazainosine. This sum gives an expected  $\Delta G$  for **2** binding of

$-15.5$  kcal/mol or a dissociation constant of 5 pM, fully consistent with the observed displacement curve (Figure 7).

## DISCUSSION

**Energetics of Transition State Analogue Binding.** The physiologically relevant interaction of Immucillins with human PNP is the first catalytic site since full catalytic inhibition occurs when the first site is filled (9). Although the binding is too tight to permit analytical ITC titration analysis, substoichiometric titrations give  $\Delta H$  values to permit calculation of  $-T\Delta S$  from known dissociation constants. The Immucillins inhibit PNP through enthalpy-driven interactions with a smaller penalty in the entropy term (Table 1). The best transition state analogue inhibitors optimize binding at the first catalytic site through the formation of specific hydrogen bond and ionic interactions. Crystal structures of the trimeric bovine PNP with Immucillin-H (**2**) and phosphate reveal at least six new hydrogen bonds and/or ionic interactions compared to the complex with isosteric substrate analogues (11). As each of these interactions is expected to be worth  $\sim 2$  kcal/mol ( $\sim 12$  kcal/mol total), they readily account for the difference in substrate and transition state binding energy, even with large entropic losses. Entropic penalties for ligand binding can include loss of dynamic flexibility in the inhibitor and/or protein scaffolds and/or altered solvent order and hydrophobic interactions. In summary, crystallographic data support enthalpic interactions with **2** by favorable hydrogen bonds and an ion pair interaction between the oxygen anion of the phosphate molecule and N4' of the iminoribitol ring ((11) and Protein Data Bank entry 1rr6).

The entropy changes vary from significantly unfavorable (Immucillins **1–9**) to near zero (**10–12**) and slightly favorable (**13–17**) with inhibitors of closely related chemical structures. The entropic pattern suggests that the entropic term originates in protein dynamic structure rather than the conformational flexibility states of the inhibitors or the order parameters for water. Changes in water order upon binding of these chemically similar inhibitors are thought to be less likely than altered protein order parameters.



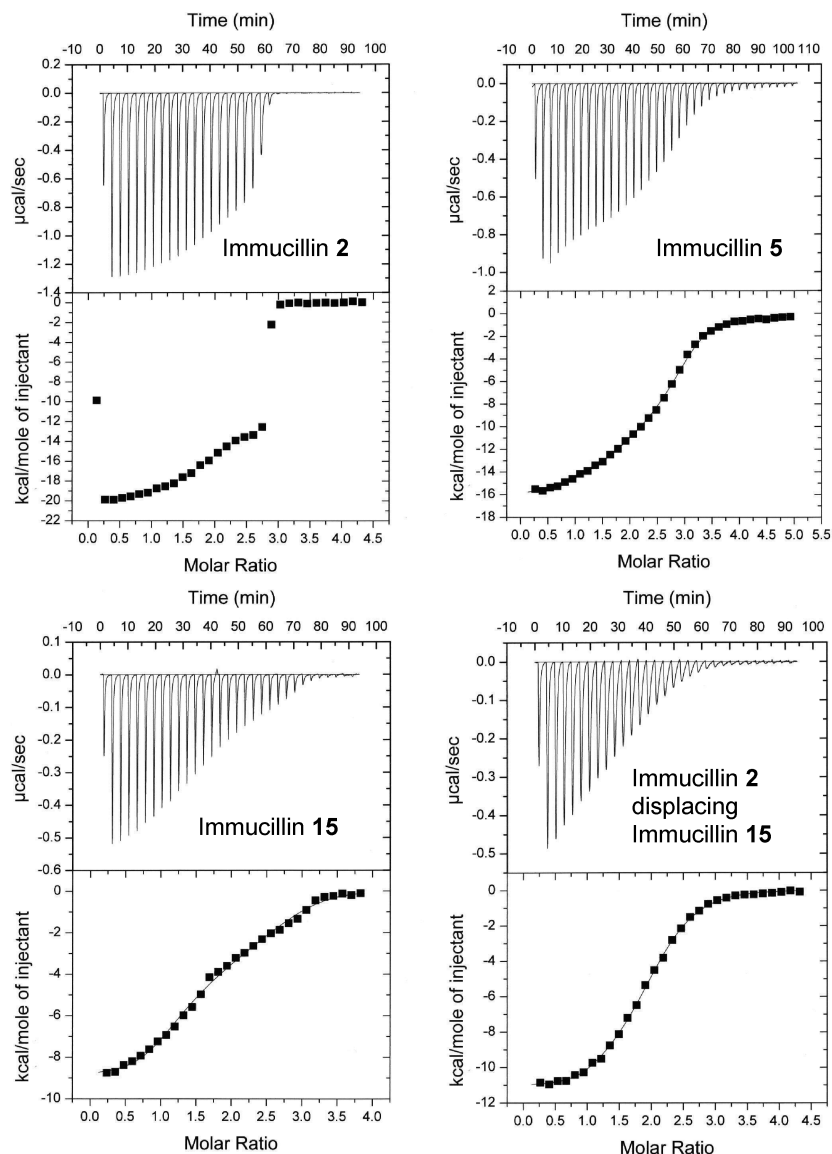


FIGURE 6: Full-saturation titrations of human PNP with select Immucillins. Immucillin **2** binds too tightly to the enzyme to permit analytically meaningful fits to three cooperative sites, but the negative cooperativity in enthalpy is apparent in altered  $\Delta H$  values as the first, second, and third sites are filled. Titrations of Immucillins **5** and **15** were fit to the equation for three sequential sites, with thermodynamic parameters for the first site filling fixed using the values from Table 1. Thermodynamic parameters for filling of sites 2 and 3, together with those for the first site (from Table 1), are listed in Table 2. Immucillin **2** displacing Immucillin **15** could be fit to an equivalent, independent sites titration curve, and the values from this displacement are listed in Table 2. The apparent dissociation constant for binding of Immucillin **2** to PNP saturated with **15** was determined by the equations for competitive binding at independent sites. The PNP trimer concentration was  $9.6 \mu\text{M}$ , and that of free Immucillin **15** at the start of the titration was  $6.3 \mu\text{M}$ . The  $K_d$  value for Immucillin **15** is assumed to be  $402 \text{ nM}$ , the dissociation constant for third-site filling for this ligand (Table 2).

**Entropy–Enthalpy Compensation.** Depending on the affinity of the Immucillins, a decreased entropic term reveals an enthalpy–entropy compensation pattern such that, with a few exceptions, the larger the  $\Delta H$  of inhibitor binding, the larger the entropic penalty for binding (Figure 5). Exceptions to the entropy–enthalpy compensation include **4**, **6**, and **8**, all exhibiting a smaller-than-expected entropic penalty for their large enthalpic driving forces. Each of these has more intrinsic flexibility (rotatable bonds) than **2** does, suggesting that inhibitor molecule flexibility is an advantage in maintaining entropic disorder in the PNP·inhibitor complex relative to the more chemically rigid **2** (Table 1).

**Effect of the 5'-Hydroxyl Group.** Compounds **11–17** depart from the others by binding with favorable entropy values to the first site (Table 1). A common feature of these is the lack of a 5'-hydroxyl group in the appropriate geometry to mimic that of

the normal substrate and the tight-binding transition state analogues. The 5'-hydroxyl group is proposed (from mutational and computational studies) to be involved in reaction coordinate motion in PNP by orbital steering from its contact with His257 (7, 11). The 5'-hydroxyl neighboring group participation is proposed to act in a promoting vibration to delocalize bonding electrons from the ribosyl group (27). The favorable entropy components of inhibitors **11–17** suggest that catalytic site and perhaps neighboring protein motion are organized by the 5'-hydroxyl interaction and that without it, more protein motion occurs, preserving a favorable entropic component. This interaction may not be so apparent in Immucillin **17**, which appears to have an intact 5'-hydroxyl (Table 1). However, this ribosyl analogue is in the L-configuration, placing the 5'-hydroxyl group in the wrong position with respect to the 9-deazaadenine ring and His257 when bound. Despite the favorable entropic terms for

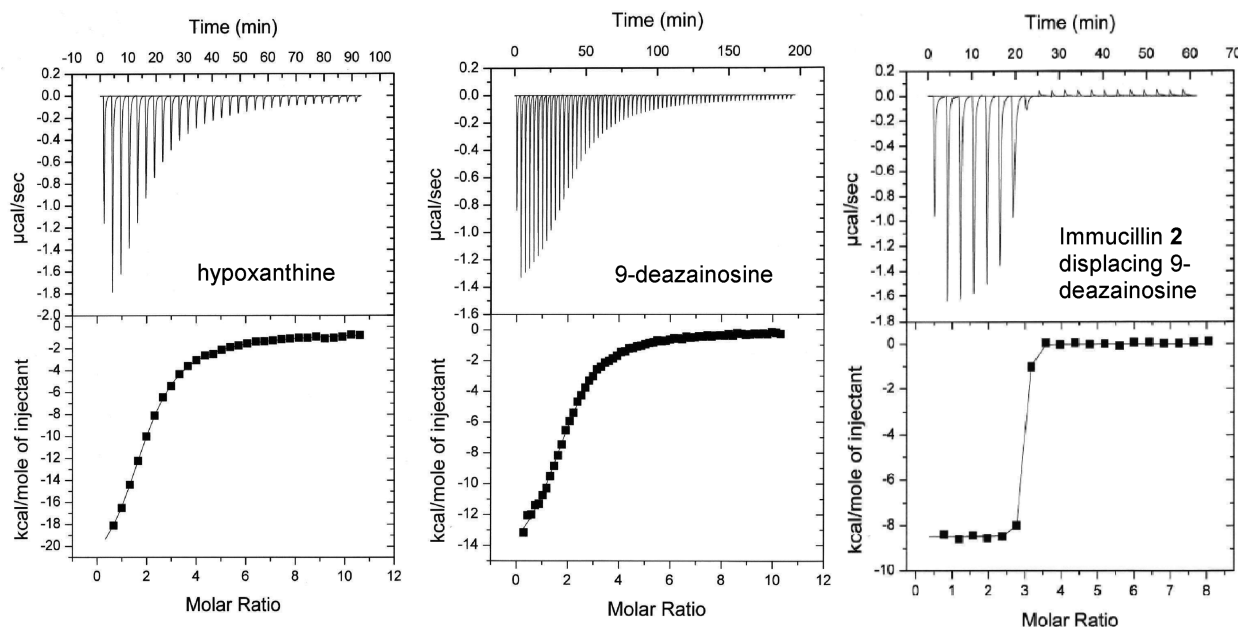
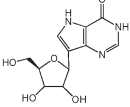
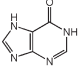


FIGURE 7: Titrations of human PNP with 9-deazainosine and hypoxanthine and displacement of 9-deazainosine with Immucillin **2**. The titration curves for hypoxanthine and 9-deazainosine were fit to the one-set-of-sites model. 9-Deazainosine (left) and hypoxanthine (middle) bind to two sites with equal affinity and thermodynamic parameters. The stoichiometry of two sites per trimer (Table 3) indicates enthalpically silent or no binding of hypoxanthine or 9-deazainosine to the third site. Displacement of 9-deazainosine by Immucillin **2** establishes tight binding at all three sites with a  $\Delta\Delta H$  of  $-8.4$  kcal/mol as 9-deazainosine is displaced. In the displacement (right panel), the PNP trimer concentration was  $10\ \mu\text{M}$  ( $30\ \mu\text{M}$  monomer concentration) and the 9-deazainosine concentration at the start of the displacement titration was  $170\ \mu\text{M}$ .

Table 3: Thermodynamics for Binding of 9-Deazainosine and Hypoxanthine to Human PNP<sup>a</sup>

9-Deazainosine 	N (Stoichiometry)	$1.98 \pm 0.017$
	$K_d$ ( $\mu\text{M}$ )	$5.4 \pm 0.2$
	$\Delta G$ (kcal/mol)	$-7.2 \pm 0.03$
	$\Delta H$ (kcal/mol)	$-15.9 \pm 0.2$
	$-T\Delta S$ (kcal/mol)	$8.7 \pm 0.2$
Hypoxanthine 	N	$1.72 \pm 0.071$
	$K_d$ ( $\mu\text{M}$ )	$4.3 \pm 0.3$
	$\Delta G$ (kcal/mol)	$-7.4 \pm 0.1$
	$\Delta H$ (kcal/mol)	$-30.5 \pm 1.6$
	$-T\Delta S$ (kcal/mol)	$23.1 \pm 1.6$

<sup>a</sup> ITC titrations were conducted in  $50\ \text{mM}\ \text{KH}_2\text{PO}_4$  at pH 7.4 and  $27\ ^\circ\text{C}$ , and the data were fit using the one-set-of-sites model provided in Origin 7.0.

these compounds, the relatively large loss in enthalpy that occurs with the incomplete ribocation mimics in **11–17** results in weaker  $\Delta G$  values for binding of these compounds.

The specific effect of the interaction of His257 with the 5'-hydroxyl group is evident by comparing Immucillins **2** and **16** which differ only by the presence of the 5'-hydroxyl group. The removal of the 5'-hydroxyl causes the  $\Delta G$  for binding to become more positive by  $3.7$  kcal/mol, the sum of the enthalpic and entropic contributions. However, the  $-T\Delta S$  term becomes  $9.0$  kcal/mol more favorable, interpreted as a large contribution from increased protein dynamics because of the lost interaction with His257.

**Negative Cooperativity in Binding.** The Immucillins bind human PNP in a negative cooperative manner so that binding to the first site hinders binding at the second and third sites. For Immucillin **5**, the entropic penalties are paid on binding to the first two sites with small but favorable entropy for binding at the third site. In contrast, the enthalpy for **15** binding to the first two sites is large and favorable and decreases at the third site. In all three sites, the entropic value is favorable. The relatively hydrophobic pyrrole

placement into the catalytic site is likely to involve favorable hydrophobic changes and to permit dynamic motion of the protein since all three hydroxyl groups found in Immucillin **2** are missing.

Filling the three binding sites alters the cooperative nature and affinity of the PNP trimer for a transition state analogue. Thus, PNP saturated with Immucillin **15** changes the  $K_d$  for all binding of Immucillin **2** to  $12\ \text{nM}$ , compared to that for first-site binding of  $56\ \text{pM}$ . Immucillin **5** binding changes from  $1.8$  to  $667\ \text{nM}$  as the three catalytic sites are filled. The structural basis for catalytic site cooperativity is likely to involve a catalytic site loop called the Phe159 loop, a flexible loop that must be open for substrates to bind and closes over the PNP Michaelis complex, to help stabilize and exclude water from the catalytic site region (12, 28). The Phe159 loop is the only part of the catalytic site contributed by the neighboring subunit and creates a physical link between subunit cooperativity and ligand binding.

**Noncooperative Substrate Analogue and Product Binding.** The substrate analogue 9-deazainosine binds independently to the first two catalytic sites and is strongly enthalpy-driven with a large entropic penalty. In contrast to transition state analogues,

9-deazainosine is unable to form a ribocation ion pair mimic with the phosphate anion but retains the 2'-, 3'-, and 5'-hydroxyl groups, all of which form H-bonds in the catalytic sites. The binding of N9-substituted guanine-based PNP inhibitors has been reported to exhibit similar thermodynamics. For these, micromolar  $K_d$  values are composed of weak enthalpic forces ( $\Delta H = -6.3$  kcal/mol for binding ganciclovir) or are entropically driven as in the cases of acyclovir ( $\Delta G = -6.7$  kcal/mol;  $-T\Delta S = -5.2$  kcal/mol) and 9-benzylguanine ( $\Delta G = -7.8$  kcal/mol;  $-T\Delta S = -4.2$  kcal/mol) (29).

Binding of hypoxanthine to PNP in phosphate is remarkably exothermic with a  $\Delta H$  of  $-30.5$  kcal/mol. Enthalpy changes of this magnitude are usually observed in tightly bound complexes such as the binding of biotin to streptavidin where the enthalpy change is  $-28.6$  kcal/mol (30). Binding of hypoxanthine is, however, modest with a large  $-T\Delta S$  of  $23.1$  kcal/mol giving a  $K_d$  of  $4.3$   $\mu$ M. These values are unlikely to tell the full story of hypoxanthine binding, since 2 mol of hypoxanthine per trimer is isolated with purified PNP and charcoal treatment is required to remove the tightly bound hypoxanthine.

Weigus-Kutrowska and associates reported hypoxanthine binding to calf spleen PNP in the absence of phosphate to be highly exothermic ( $\Delta H = -14.3$  kcal/mol), but the status of tightly bound hypoxanthine in these preparations is unknown (31). Hypoxanthine forms H-bonds with Glu201 and Asp243, and its binding also removes this planar, hydrophobic molecule from solvent and places it in a hydrophobic environment near Phe200, Val245, Val217, and Met219 and near Phe159 [contributed by the neighboring subunit (11, 12)]. As hydrophobic interactions would contribute to a favorable entropic term and the observed entropy is highly unfavorable, the thermodynamic profile indicates that the binding energy comes primarily from the favorable leaving group interactions. The entropic penalty of hypoxanthine binding is therefore likely to reside in increased order parameters for the protein.

Why should transition state analogues exhibit strong cooperativity while the substrate analogue and product do not? We can speculate that protein conformational collapse around the transition state analogues, structurally identified by at least six new hydrogen and/or ionic bonds relative to ground state ligands, transmits a structural change via the Phe159 loop, contributed by the neighboring subunit. This reflects the nature of the transition state. In contrast, loose interactions of the Michaelis complexes do not involve tight interactions and do not transmit conformational rigidity to neighboring subunits. Experimental evidence supporting this proposal comes from hydrogen–deuterium exchange in bovine PNP with Immucillin 2 and phosphate bound. Filling of one catalytic site decreased H–D exchange rates in all three subunits (32).

**Comparison of Immucillins with Other Inhibitors.** Thermodynamic studies of well-characterized systems, including the binding of statins to HMG-CoA reductase and the binding of presumptive transition state analogue inhibitors to HIV-1 protease, were conducted. These inhibitors bind with  $\Delta G$  values ranging from  $-9.0$  to  $-14.9$  kcal/mol (22, 33–35) (Figure 8). For the  $13$  pM experimental HIV-1 protease inhibitor KNI-10033, the tetrahedral carbon alcohol mimics the intermediate of this aspartyl protease, contributing to favorable enthalpy, and the multiple hydrophobic groups of protease inhibitors (exemplified here by KNI-10033) contribute to favorable entropic interactions. This combination provides a remarkable  $\Delta G$  of  $-14.9$  kcal/mol.

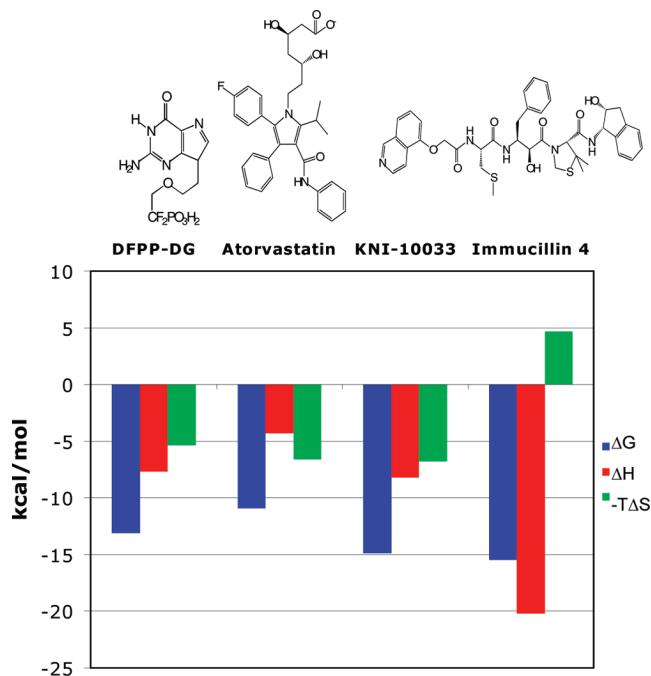


FIGURE 8: Thermodynamic inhibitor signatures for comparison with Immucillin 4. DFPP-DG is a bisubstrate analogue of bovine PNP; Atorvastatin (Lipitor) is an inhibitor of HMG-CoA reductase, and KNI-10033 is an experimental tight-binding ( $13$  pM) inhibitor of HIV-1 protease. DFPP-DG, Atorvastatin, and KNI-10033 bind their respective targets with similar contributions from the enthalpy and entropy terms. Immucillin 4 exhibits a larger enthalpy contribution to binding but an entropy penalty. Despite the entropic penalty, the enthalpic elements of transition state binding give it the greatest affinity of these ligands.

The statins are powerful inhibitors of HMG-CoA reductase in wide use for mediation of blood cholesterol levels. Titration of a type 1 statin (pravastatin) and four type 2 statins (fluvastatin, cerivastatin, atorvastatin, and rosuvastatin) with HMG-CoA reductase gave  $K_i$  values of  $2.3$ – $256$  nM with enthalpy values ranging from zero to  $-9.3$  kcal/mol (33). Thus, the entropic term contributes significantly to all of these interactions. Structures of these drugs include multiple hydrophobic groups, consistent with the favorable entropic partition of the drugs from water to the relative hydrophobic site of HMG-CoA reductase. Energetics of Atorvastatin (Lipitor) binding (Figure 8) exemplify the thermodynamics of statin binding, with the  $-10.9$  kcal/mol  $\Delta G$  value consisting of a favorable  $\Delta H$  of  $-4.3$  kcal/mol and a favorable  $T\Delta S$  term contributing even more energy ( $-6.6$  kcal/mol). Thermodynamic analysis of five statins led to the conclusion that binding affinity is correlated with binding enthalpy and the most powerful statins bind with the strongest enthalpies (33).

The tightest-binding Immucillins for human PNP are powerfully driven by unusually large enthalpy terms, in several cases, greater than  $-20$  kcal/mol. Thermodynamic interactions of Immucillin 4 compared with Atorvastatin (Lipitor) and KNI-10033 demonstrate the exceptional enthalpy of binding (Figure 8). Entropic penalties in the binding of transition state analogues are unavoidable since the analogues convert the dynamic motions of catalysis into more static binding energy, thus causing substantial increases in protein structural order parameters (36). In contrast to the entropic penalty for Immucillin 4, the substrate analogue DFPP-DG binds with a favorable entropy component, but without the interactions of transition state analogues, it suffers in the enthalpic term.

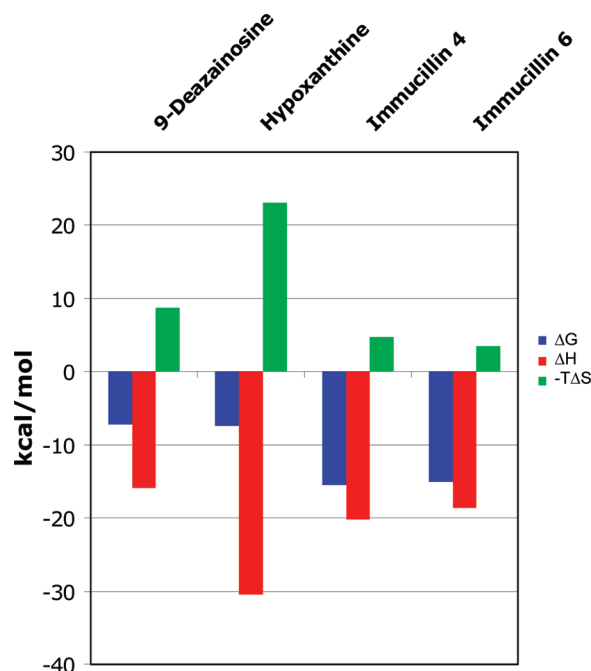


FIGURE 9: Thermodynamic signatures for binding of 9-deazainosine, hypoxanthine, and Immucillins **4** and **6** to human PNP. The bars represent  $\Delta G$  (blue),  $\Delta H$  (red), and  $-T\Delta S$  (green). The thermodynamic profiles for Immucillins **4** and **6** were taken from the single-subunit titration study (Table 1). The signatures for the substrate analogue inhibitor and product are less favorable for binding, and although the enthalpy terms are large, they are compensated by large entropic penalties. These are interpreted as protein organization changes. Immucillins **4** and **6** exhibit thermodynamic signatures marked by more favorable  $\Delta G$  values due to larger enthalpy changes and small entropy penalties.

We know of no other collection of transition state analogues or inhibitors designed by any method that match the large, enthalpy-driven binding features of the interactions of Immucillin with PNP. Thermodynamic results support an unusual ability to capture the energetic interactions leading to transition state formation. A fortunate feature of transition state analogue design for PNP is the contrast between the electronically neutral substrates (inosine and guanosine) and the cationic transition states. Thus, the ability to mimic the cationic transition state in stable analogues and to form an ion pair with phosphate at the catalytic sites provides a major contribution to the large enthalpic values for binding of analogues to PNP. One specific example of the transition state cation effect is the difference in binding of Immucillin **2** and 9-deazainosine, where the replacement of a single atom, the 4'-nitrogen cation with the 4'-neutral oxygen, changes the binding affinity from 56 pM to 5.4  $\mu$ M, a decrease in binding affinity of a factor of nearly  $10^5$ .

**Entropy–Enthalpy Compensation.** A cruel fact of inhibitor design is that every favorable hydrogen bond or ionic interaction added into a catalytic site inhibitor ligand stabilizes the complex and adds unfavorable entropic contributions to binding. Building flexibility into inhibitors that preserve the motion of the protein while maximizing the hydrogen bond and ionic interactions between the inhibitor and the catalytic site is one way to minimize the entropic penalty. Immucillin **8** contains the three hydroxyl groups present on a ribosyl group or on Immucillin **2**, and also the ribocation mimic in the amine functionality. These interactions generate an impressive  $\Delta H$  of  $-17.5$  kcal/mol while only paying a  $-T\Delta S$  penalty of 2.3 kcal/mol to give a dissociation constant of 8.6 pM. Likewise,

Immucillins **4** and **6** have modest entropic penalties (especially when compared to hypoxanthine or 9-deazainosine binding) with large enthalpy values generated from the favorable features of transition state mimicry (Figure 9). Transition state analogues for mammalian PNPs with binding constants of  $< 10$  pM have been termed “the ultimate inhibitors” because a single inhibitor treatment in mice saturates the target PNP and maintains functional inhibition for the lifetime of erythrocytes [25 days in mice (37)].

## CONCLUSIONS

High affinity, specificity, and lack of toxicity have made the Immucillins candidates for clinical studies in T-cell-related disorders. The tight binding of these analogues to the first subunit on human PNP is characterized by an enthalpy change as large as  $-22.7$  kcal/mol. Tight binding of the transition state analogues comes with entropy penalties interpreted as increased order parameters in the PNP–inhibitor complexes. As transition state features are eliminated from the inhibitors, binding affinity decreases and the entropic penalty decreases and becomes favorable for binding with weaker inhibitors. Tight binding to 8.5 pM occurs when the features of the transition state are preserved in inhibitor design, but flexibility is built into the transition state analogue, presumably, to permit increased dynamic flexibility in the enzyme–inhibitor complex.

## REFERENCES

- Giblett, E. R., Ammann, A. J., Wara, D. W., Sandman, R., and Diamond, L. K. (1975) Nucleoside-phosphorylase deficiency in a child with severely defective T-cell immunity and normal B-cell immunity. *Lancet* **1**, 1010–1013.
- Ravandi, F., and Gandhi, V. (2006) Novel purine nucleoside analogues for T-cell lineage acute lymphoblastic leukaemia and lymphomas. *Expert Opin. Invest. Drugs* **12**, 1601–1613.
- Lewandowicz, A., and Schramm, V. L. (2004) Transition state analysis for human and *Plasmodium falciparum* purine nucleoside phosphorylases. *Biochemistry* **43**, 1458–1468.
- Evans, G. B., Furneaux, R. H., Lewandowicz, A., Schramm, V. L., and Tyler, P. C. (2003) Exploring structure-activity relationships of transition state analogues of human purine nucleoside phosphorylase. *J. Med. Chem.* **46**, 3412–3423.
- Taylor, E. A., Clinch, K., Kelly, P. M., Li, L., Evans, G. B., Tyler, P. C., and Schramm, V. L. (2007) Acyclic riboxocarbenium ion mimics as transition state analogues of human and malarial purine nucleoside phosphorylases. *J. Am. Chem. Soc.* **129**, 6984–6985.
- Mason, J. M., Murkin, A. S., Li, L., Schramm, V. L., Gainsford, G. J., and Skelton, B. W. (2008) A  $\beta$ -fluoroamine inhibitor of purine nucleoside phosphorylase. *J. Med. Chem.* **51**, 5880–5884.
- Murkin, A. S., Clinch, K., Mason, J. M., Tyler, P. C., and Schramm, V. L. (2008) Immucillins in custom catalytic-site cavities. *Biorg. Med. Chem. Lett.* **18**, 5900–5903.
- Kline, P. C., and Schramm, V. L. (1993) Purine nucleoside phosphorylase. Catalytic mechanism and transition-state analysis of the arsenolysis reaction. *Biochemistry* **32**, 13212–13219.
- Miles, R. W., Tyler, P. C., Furneaux, R. H., Bagdasarian, C. K., and Schramm, V. L. (1998) One-third-the-sites transition-state inhibitors for purine nucleoside phosphorylase. *Biochemistry* **37**, 8615–8621.
- Lewandowicz, A., Ringia Taylor, E. A., Ting, L., Kim, K., Tyler, P. C., Evans, G. B., Zubkova, O. V., Mee, S., Painter, G. F., Lenz, D. H., Furneaux, R. H., and Schramm, V. L. (2005) Energetic mapping of transition state analogue interactions with human and *Plasmodium falciparum* purine nucleoside phosphorylases. *J. Biol. Chem.* **280**, 30320–30328.
- Fedorov, A., Shi, W., Kicska, G., Fedorov, E., Tyler, P. C., Furneaux, R. H., Hanson, J. C., Gainsford, G. J., Larese, J. Z., Schramm, V. L., and Almo, S. C. (2001) Transition state structure of purine nucleoside phosphorylase and principles of atomic motion in enzymatic catalysis. *Biochemistry* **40**, 853–860.
- Mao, C., Cook, W. J., Zhou, M., Federov, A. A., Almo, S. C., and Ealick, S. E. (1998) Calf spleen purine nucleoside phosphorylase



- complexed with substrates and substrate analogues. *Biochemistry* 37, 7135–7146.
13. De Azevedo, W. F. Jr., Canduri, F., Dos Santos, D. M., Silva, R. G., De Oliveira, J. S., De Carvalho, L. P., Basso, L. A., Mendes, M. A., Palma, M. S., and Santos, D. S. (2003) Crystal structure of human purine nucleoside phosphorylase at 2.3 Å resolution. *Biochem. Biophys. Res. Commun.* 308, 545–552.
  14. Breer, K., Wielgus-Kutrowska, B., Hashimoto, M., Hikishima, S., Yokomatsu, T., Szczepanowski, R. H., Bochtler, M., Girstun, A., Staron, K., and Bzowska, A. (2008) Thermodynamic studies of interactions of calf spleen PNP with acyclic phosphonate inhibitors. *Nucleic Acids Symp. Ser.* 52, 663–664.
  15. Ghanem, M., Saen-oon, S., Zhadin, N., Wing, C., Cahill, S. M., Schwartz, S. D., Callender, R., and Schramm, V. L. (2008) Tryptophan-free human PNP reveals catalytic site interactions. *Biochemistry* 47, 3202–3215.
  16. Evans, G. B., Furneaux, R. H., Tyler, P. C., and Schramm, V. L. (2003) Synthesis of a transition state analogue inhibitor of purine nucleoside phosphorylase via the Mannich reaction. *Org. Lett.* 5, 3639–3640.
  17. Lim, M.-I., Ren, Y.-Y., Otter, B. A., and Klein, R. S. (1983) Synthesis of “9-deazaguanosine” and other new pyrrolo[3,2-d]pyrimidine C-nucleosides. *J. Org. Chem.* 48, 780–788.
  18. Morrison, J. F., and Walsh, C. T. (1988) The behavior and significance of slow-binding enzyme inhibitors. *Adv. Enzymol. Relat. Areas Mol. Biol.* 61, 201–301.
  19. Zhang, Y., and Zhang, Z. (1998) Low-affinity binding determined by titration calorimetry using a high-affinity coupling ligand: A thermodynamic study of ligand binding to protein tyrosine phosphatase 1B. *Anal. Biochem.* 261, 139–148.
  20. Sigurskjold, B. W. (2000) Exact analysis of competition ligand binding by displacement isothermal titration calorimetry. *Anal. Biochem.* 277, 260–266.
  21. Williams, D. H., Stephens, E., O’Brien, D. P., and Zhou, M. (2004) Understanding noncovalent interactions: Ligand binding energy and catalytic efficiency from ligand-induced reductions in motion within receptors and enzymes. *Angew. Chem., Int. Ed.* 43, 6596–6616.
  22. Lafont, V., Armstrong, A. A., Ohtaka, H., Kiso, Y., Amzel, L. M., and Freire, E. (2007) Compensating enthalpic and entropic changes hinder binding affinity optimization. *Chem. Biol. Drug Des.* 69, 413–422.
  23. Cole, J. L., and Garsky, V. M. (2001) Thermodynamics of peptide inhibitor binding to HIV-1 gp41. *Biochemistry* 40, 5633–5641.
  24. Eastberg, J. H., Smith McConnell, A., Zhao, L., Ashworth, J., Shen, B. W., and Stoddard, B. L. (2007) Thermodynamics of DNA target site recognition by homing endonucleases. *Nucleic Acids Res.* 35, 7209–7221.
  25. Olsson, T. S. G., Williams, M. A., Pitt, W. R., and Ladbury, J. E. (2008) The thermodynamics of protein-ligand interaction and solvation: Insights for ligand design. *J. Mol. Biol.* 384, 1002–1017.
  26. Kline, P. C., and Schramm, V. L. (1992) Purine nucleoside phosphorylase. Inosine hydrolysis, tight binding of the hypoxanthine intermediate and third-site reactivity. *Biochemistry* 31, 5964–5973.
  27. Saen-oon, S., Ghanem, M., Schramm, V. L., and Schwartz, S. D. (2008) Remote mutations and active site dynamics correlate with catalytic properties of purine nucleoside phosphorylase. *Biophys. J.* 94, 4078–4088.
  28. Pugmire, M. J., and Ealick, S. E. (2002) Structural analyses reveal two distinct families of nucleoside phosphorylases. *Biochem. J.* 361, 1–25.
  29. Todorova, N. A., and Schwarz, F. P. (2008) Effect of the phosphate substrate on drug-inhibitor binding to human purine nucleoside phosphorylase. *Arch. Biochem. Biophys.* 480, 122–131.
  30. Hyre, D. E., Le Trong, I., Freitag, S., and Stenkamp, R. E. (2000) Ser45 plays an important role in managing both the equilibrium and transition state energetics of the streptavidin-biotin system. *Protein Sci.* 9, 878–885.
  31. Wielgus-Kutrowska, B., Frank, J., Holy, A., Koellner, G., and Bzowska, A. (2003) Interactions of trimeric purine nucleoside phosphorylase with ground state analogues-calorimetric and fluorimetric studies. *Nucleosides, Nucleotides Nucleic Acids* 22, 1695–1698.
  32. Wang, F., Miles, R. W., Kicska, G., Nieves, E., Schramm, V. L., and Angeletti, R. H. (2000) Immucillin-H binding to purine nucleoside phosphorylase reduces dynamic solvent exchange. *Protein Sci.* 9, 1660–1668.
  33. Carbonell, T., and Freire, E. (2005) Binding thermodynamics of statins to HMG-CoA reductase. *Biochemistry* 44, 11741–11748.
  34. Sarver, R. W., Bills, E., Bolton, G., Bratton, L. D., Caspers, N. L., Dunbar, J. B., Harris, M. S., Hutchings, R. H., Kennedy, R. M., Larsen, S. D., Pavlovsky, A., Pfefferkorn, J. A., and Bainbridge, G. (2008) Thermodynamic and structure guided design of statin based inhibitors of 3-hydroxy-3-methylglutaryl coenzyme A reductase. *J. Med. Chem.* 51, 3804–3813.
  35. Velazquez-Campoy, A., Kiso, Y., and Freire, E. (2001) The binding energetics of first- and second-generation HIV-1 protease inhibitors: Implications for drug design. *Arch. Biochem. Biophys.* 390, 169–175.
  36. Schramm, V. L. (2005) Enzymatic transition states: Thermodynamics, dynamics and analogue design. *Arch. Biochem. Biophys.* 433, 13–26.
  37. Lewandowicz, A., Tyler, P. C., Evans, G., Furneaux, R. H., and Schramm, V. L. (2003) Achieving the ultimate physiological goal in transition state analogue inhibitors for purine nucleoside phosphorylase. *J. Biol. Chem.* 278, 31465–31468.
  38. Rinaldo-Matthis, A., Murkin, A. S., Ramagopal, U. A., Clinch, K., Mee, S. P. H., Evans, G. B., Tyler, P. C., Furneaux, R. H., Almo, S. C., and Schramm, V. L. (2008) L-Enantiomers of transition state analogue inhibitors bound to human purine nucleoside phosphorylase. *J. Am. Chem. Soc.* 130, 842–844.
  39. Ringia Taylor, E. A., Tyler, P. C., Evans, G. B., Furneaux, R. H., Murkin, A. S., and Schramm, V. L. (2006) Transition state analogue discrimination by related purine nucleoside phosphorylases. *J. Am. Chem. Soc.* 128, 7126–7127.